

SThM-based local thermomechanical analysis: Measurement intercomparison and uncertainty analysis

Eloise Guen^a, Petr Klapetek^{b,c}, Robert Puttock^{d,f}, Bruno Hay^e, Alexandre Allard^e, Tony Maxwell^d, Pierre-Olivier Chapuis^a, David Renahy^a, Guillaume Davee^e, Miroslav Valtr^{b,c}, Jan Martinek^{b,g}, Olga Kazakova^d, Séverine Gomès^{a,*}

^a CETHIL UMR5008, Univ Lyon, CNRS, INSA-Lyon, Université Claude Bernard Lyon 1, F-69621, Villeurbanne, France

^b Czech Metrology Institute, Okružní 31, 638 00, Brno, Czech Republic

^c CEITEC, Brno University of Technology, Purkyňova 123, 612 00, Brno, Czech Republic

^d National Physical Laboratory, Hampton Road, Teddington, Middlesex, TW11 0LW, UK

^e Laboratoire National de métrologie et d'Essais, 29 avenue Roger Hennequin, 78197, Trappes Cedex, France

^f Department of Physics, Royal Holloway University of London, Egham, TW20 0EX, UK

^g Department of Physics, Faculty of Civil Engineering, Brno University of Technology, Žitkova 17, 602 00, Brno, Czech Republic

ABSTRACT

We assess Scanning Thermal Microscopy (SThM) with a self-heated doped silicon nanoprobe as a method for determining the local phase transition temperature of polymeric materials by means of nano-thermomechanical analysis (nano-TA). Reference semi-crystalline samples and amorphous test samples, characterized first using differential scanning calorimetry (DSC), are studied by nano-TA in the temperature range 50–250 °C. The repeatability, the reproducibility and the reliability of nano-TA are evaluated by three laboratories by applying the same calibration protocol prior to and after the measurements. The calibration of the probe temperature scale and the variability of the sample thermomechanical response are validated by Monte Carlo uncertainty analysis, resulting in a calculated uncertainty between 3 and 5 K. The SThM probe temperature data represented as a function of DSC-measured phase-transition temperatures of the semi-crystalline samples rule out the possibility of a quadratic fit and call for a linear calibration in absence of additional information. The maximum deviation obtained between SThM and DSC temperatures with such linear calibration reaches ± 30 K for melting temperatures and 50 K for glass transition temperatures.

1. Context and goal

The manufacturing and microelectronics industries have acknowledged a strong need to develop methodologies to characterize polymer-based composites with improved spatial resolution, in particular for the determination of mechanical, electrical and thermal properties. Indeed the overall performances of the composites, including fibre-reinforced polymers, blends, nanotubes and their co-related polymer based composites, and multi-layer systems can be strongly affected by the development of interphase regions with properties differing from the properties of the constituent materials [1,2]. Moreover, the physical properties of composites can be tuned by the chemical functionalization of filler surface [3]. Therefore, interphases between the fillers and the polymer matrix have a significant contribution to the physical properties of composites. However, because of the relatively small volume of the

interfacial region compared to that of the bulk material, conventional analytical techniques are unsuitable for elucidation of the interfacial microstructure and properties.

Local analysis may be addressed by techniques involving interface spectroscopic or mechanical measurements with some forms of microscopy such as *atomic force microscopy* (AFM), *Raman microscopy* or *near infrared microscopy*. In this work, we analyse the use of *Scanning Thermal Microscopy* (SThM) as a method for local thermal measurement, in particular phase change temperature measurements. SThM is a mode of scanning probe microscope where the conventional AFM probe is replaced by a probe equipped with a miniaturised thermal sensor [4]. For the simplest mode of local thermomechanical analysis (L-TMA), the thermal sensor is electrically resistive so that the tip can be self-heated by Joule effect. After thermal calibration, the probe is first pressed against a chosen region of the sample, leading to deflection of the

* Corresponding author. CETHIL, Domaine Scientifique de la DOUA, INSA de Lyon, Bâtiment Sadi Carnot, 9 rue de la Physique, 69621, Villeurbanne Cedex, France.

E-mail addresses: eloise.guen@insa-lyon.fr (E. Guen), pklapetek@cmi.cz (P. Klapetek), robb.puttock@npl.co.uk (R. Puttock), bruno.hay@lne.fr (B. Hay), Alexandre.allard@lne.fr (A. Allard), tony.maxwell@npl.co.uk (T. Maxwell), pierre-olivier.chapuis@insa-lyon.fr (P.-O. Chapuis), david.renahy@univ-lyon1.fr (D. Renahy), guillaume.davee@lne.fr (G. Davee), mvaltr@cmi.cz (M. Valtr), jmartinek@cmi.cz (J. Martinek), olga.kazakova@npl.co.uk (O. Kazakova), severine.gomes@insa-lyon.fr (S. Gomès).

<https://doi.org/10.1016/j.ijthermalsci.2020.106502>

Received 12 September 2019; Received in revised form 13 April 2020; Accepted 22 May 2020

Available online 30 May 2020

1290-0729/© 2020 Elsevier Masson SAS. All rights reserved.

cantilever, with a given initial force. By ramping a dc voltage through the probe, its deflection along the z-axis (perpendicular to the sample surface) is recorded. The force feedback mechanism needed for imaging is typically disabled throughout the ramp; otherwise, the z-actuator motion would drive the tip through the specimen as it softens. If the material undergoes a phase transition, its mechanical properties vary (e. g. softening), so that the tip indents the sample and the cantilever deflection changes. Monitoring of the cantilever deflection then permits the detection of phase transitions. Phase changes such as glass transition, melting and softening of polymers can be detected and the associated phase change temperatures estimated [5–7].

L-TMA was first proposed by Hammiche et al. in 1996 using the SThM Wollaston wire microprobe [5,8]. Nowadays a smaller tip that consists in doped silicon nanoprobe (DS probe) with a higher spatial resolution on the sub-100 nm scale is used [6,9,10]. The phase change temperatures using nanometer-scale thermal analysis (nano-TA) of various polymeric materials including thin films on substrates [6,11] and polymer-based composites such as mixed-phase polymeric materials [12] or polymers reinforced with micro or nanostructures [10,13] have already been measured. However, numerous sources of uncertainty on the measurement have been identified [14] and there is a lack of metrological approach for this type of analysis.

In this context, the objective of this work is to assess the performance of the nano-TA method according to standard ISO 5725-2. The results provide an evaluation of the trueness and precision of the method, with an associated uncertainty. The ISO 5725-2 standard guides the organization of a comparison between measurements and the evaluation of a maximized value of uncertainty, which includes laboratory effects, associated to a given measurement method. The comparisons of the SThM data gathered three laboratories applying the same measurement protocol. It was then possible to evaluate the method with the following parameters:

- (i) the repeatability, which indicates the dispersion of the data within the same laboratory, in a short time interval, when obtained by the same operator,
- (ii) the reproducibility, which is the result of the dispersion of the data when obtained in different laboratories with different equipment and different operators.

After agreement of the calibration and measurement protocols, specific reference samples were prepared for all participating laboratories, which performed their measurements in blind conditions (without knowing the results obtained by the other partners). A protocol for the organisation of blind comparison related to the nano-TA measurements by SThM was jointly devised by the participating laboratories and can be found in Ref. [15]. The reliability of the nano-TA method is investigated here, by analysing uncertainties and by making comparisons between the results obtained in the three laboratories.

2. Experimental setups and samples

2.1. Setups

Three different SThM systems (detailed in Table 1) were used for the measurements required for the analysis of uncertainties and nano-TA measurements. All these devices comprise four main components (Fig. 1):

- an AFM using a laser-detection system to detect the motion of the cantilever,
- a doped silicon (DS) probe used simultaneously as heat source and sensor,
- an electronics module for the electrical heating of the probe and the measurement of its electrical resistance,
- a software control system.

Table 1
SThM systems

Device code	Atomic force microscope	Probe(s)	Electronics module and software control system
Device1	Dimension Icon microscope (Bruker)	VITA-NANOTA-200 and 300 probes supplied by Bruker	Developed in Czech Metrology Institute
Device2	NTEGRA-Aura microscope (NT-MDT)	VITA-NANOTA-200 probes supplied by Bruker	NanoTa module from Anasys Instruments
Device3	NanoIR2-s by Anasys Instruments	PR-EX-AN2-200 probes supplied by Anasys Instruments	NanoTa module and software from Anasys Instruments

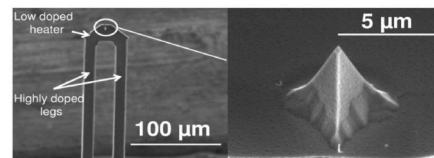
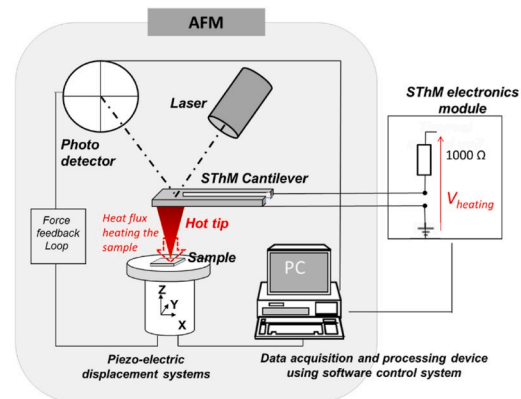


Fig. 1. Main components of equipment used for nano-TA measurements. a. SThM microscope components b. Scanning electron microscopy images of a DS probe.

As shown in Fig. 1 b, the cantilever of the DS probe consists of two micrometric legs with high doping level and a low doped resistive element platform. The tip with a nanometric curvature radius (10–30 nm) has a pyramidal shape and is mounted on top of the resistive element. These silicon-based probes are batch-fabricated. Their spring constant depends on the cantilever dimensions: $0.5\text{--}3\text{ N m}^{-1}$ and $0.5\text{--}1\text{ N m}^{-1}$ for the 300 and 200 μm -long cantilevers, respectively.

2.2. Samples

In this work, various polymeric materials were prepared as reference and test samples. The prepared sample set includes:

- Four reference bulk highly semi-crystalline polymeric materials (polycaprolactone (PCL), low-density polyethylene (LDPE), polyoxymethylene (POM) and polyethylene terephthalate (PET)) with clearly defined melting temperature T_m between $50\text{ }^\circ\text{C}$ to $250\text{ }^\circ\text{C}$. They were used for the calibration of the SPM techniques.

- Five test amorphous polymeric materials: Polyvinyl chloride (PVC), Polystyrene (PS), Polymethyl methacrylate (PMMA), Polycarbonate (PC), Polysulfone (PSU) with glass transition temperature with a clearly defined T_g between $50\text{ }^\circ\text{C}$ and $200\text{ }^\circ\text{C}$. The SThM operators did not know their properties when the nano-TA measurements were performed. They will be called “test” samples in the following.

Differential scanning calorimetry (DSC) was used for characterizing the polymer phase transition temperatures (T_m or T_g). Three repetitions

were then conducted for each specimen under nitrogen at a heating rate of 10 K/min. Table 2 and Table 3 summarise sources of the raw materials, the T_m or T_g temperatures measured by DSC and their associated expanded uncertainty ($k = 2$), and the thermal conductivity K for the calibration and test samples respectively.

From each raw material, a specimen with a surface area for SThM measurements of about 1 mm^2 was prepared using *ultramicrotomy*, involving cryogenic cutting, to produce flat surface with nanometric topography details. Roughness parameter S_q (standard height deviation) of each sample was measured using AFM in intermittent contact mode and was found between 10 and 20 nm depending on sample. As shown in Fig. 2, this ensures a much better reproducibility of the measurements and strongly reduces artefacts due to topography on the measurement that can be observed when the studied surfaces are prepared using standard *microtomy*.

A set of three samples commercialized by Anasys Instruments (now owned by Bruker) for the calibration of the nano-TA method [16] was also used for comparison with results obtained on the set of samples that we had prepared. These three samples also consist of semi-crystalline polymeric materials: PCL, high-density polyethylene (HDPE) and PET, with provided melting temperature T_m equal to $55 \text{ }^\circ\text{C}$, $116 \text{ }^\circ\text{C}$ and $235 \text{ }^\circ\text{C}$, respectively.

A silicon substrate was systematically measured between the measurements of polymeric specimens to estimate the thermal drift in the measurement set (additionally to the thermomechanical measurement for the probe out of contact with the sample) and to regularly verify probe contamination from polymer residues. For such thermally conductive materials, the amount of heat transferred from the hot tip to the sample strongly depends on the thermal resistance at the probe-sample contact [17]. Any variation in the signals measured on the silicon sample allows for detection of a change at the tip apex that can affect a measurement set. Note that Si substrates are covered with native oxide, but it is considered to grow extremely slowly in comparison to the time scale of the experiments and its impact is negligible.

3. Protocol for measurement and blind comparisons on nano-TA measurement

Experimental protocol for the inter-laboratory comparison is summarized only briefly here, showing the key points for the uncertainty analysis. The tip is placed on a location on the sample surface chosen commonly using previously acquired topographical images as a guide. A heating signal is applied at a specific rate, with the deflection of the cantilever monitored as a function of heating voltage (Figs. 1 and 3). Nano-TA is performed by placing the tip on the surface and applying a force (monitored by the bending the cantilever) by a predetermined amount in a force feedback loop. The motion of the cantilever is detected by means of the laser-detection system, while in order to prevent the z-actuator driving the tip through the sample as it melts or softens, the

Table 2
Description of the calibration samples

Material	Provider	T_m ($^\circ\text{C}$)	Expanded uncertainty ($^\circ\text{C}$)	K ($\text{W}\cdot\text{m}^{-1}\cdot\text{K}^{-1}$) ^{a, b}
Polycaprolactone (PCL)	Sigma-Aldrich	61.7	2	0.2 ^a
Low Density Polyethylene (LDPE)	Radiospares	110.4	1.2	0.33 ^a
Polyoxymethylene (POM)	Goodfellow	166.9	1.5	0.22–0.24 ^a
Polyethylene terephthalate (PET)	Goodfellow	249.3	1.9	0.265 ^b

^a From provider.

^b The expanded uncertainty associated to the determination of K at $23 \text{ }^\circ\text{C}$ is estimated to be 5%.

Table 3

Description of the test samples (“unknown samples” for nano-TA users when measurements were performed)

Material	Provider	T_g ($^\circ\text{C}$)	Expanded uncertainty ($^\circ\text{C}$)	K ($\text{W}\cdot\text{m}^{-1}\cdot\text{K}^{-1}$)
Polyvinyl chloride (PVC)	Goodfellow	65.2	6.9	0.238 ^b
Polystyrene (PS)	Goodfellow	118.0	2.4	0.1–0.13 ^a
Polymethyl methacrylate (PMMA)	Goodfellow	120.1	2.5	0.187 ^b
Polycarbonate (PC)	Goodfellow	148.8	1.9	0.221 ^b
Polysulfone (PSu)	Goodfellow	187.0	1.5	0.174 ^b

^a From provider.

^b The expanded uncertainty associated to the determination of K at $23 \text{ }^\circ\text{C}$ is estimated to be 5%.

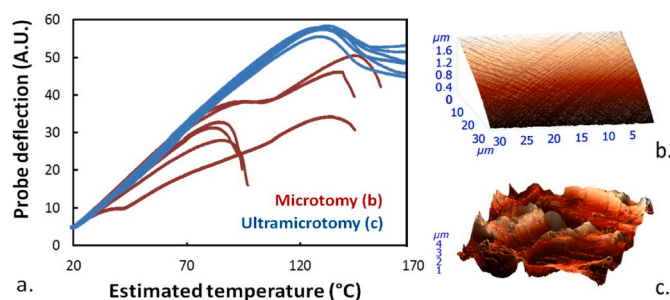


Fig. 2. (a) Probe deflection measurements for PMMA samples with two types of surfaces. (b, c) Topography images obtained by AFM of a PMMA sample surface prepared using (b) ultramicrotomy and (c) microtomy.

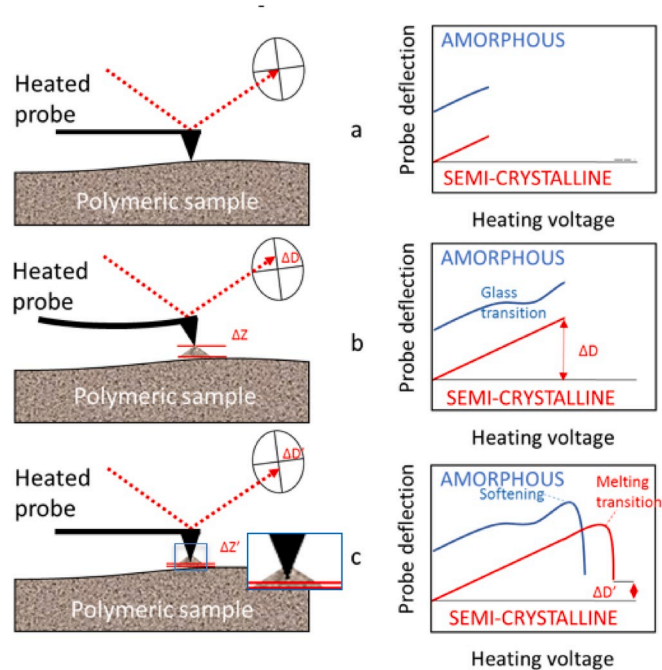


Fig. 3. Deflection curves for amorphous and semi-crystalline polymeric materials as a function of the heating voltage applied to the nano-TA probe, i.e. before calibration.

force feedback is disengaged as the thermal programme starts. As the material underneath the probe expands the force steadily increases, and the cantilever is pushed upwards (Fig. 3.b). The rate of upward movement depends on the thermal expansion coefficient, thermal

conductivity and heat capacity of the material. If a glass transition (Fig. 3.b) or a melting temperature is reached, the material beneath the probe softens; the probe penetrates the sample surface in order to dissipate the force on the cantilever (Fig. 3.c). In this manner, both the dimensional changes and thermal phase transitions in the sample are measured locally as a function of the heating voltage.

After calibration of the probe, dimensional changes can be studied as a function of the temperature allowing the measurement of phase change temperatures. The procedure follows the experimental steps suggested by Anasys Instruments [18,19]. Prior to the measurements, the temperature–heating voltage relationship is calibrated using semi-crystalline polymers with known values of melting temperature. Nano-TA measurements of these samples are performed. It is then a matter of converting the scale of the heating voltage applied to the probe into a temperature scale. The probe temperature is never equal to that of the samples, but each calibrating sample allows obtaining an apparent transition temperature as a function of probe voltage when the phase transition occurs. The whole calibration experiments therefore allow obtaining a discrete set of sample apparent transition temperatures as a function of probe voltage.

For the inter-laboratory comparison presented and discussed in this paper, we used the following protocol. Calibration and measurements were performed under ambient air conditions for a dc heating voltage ramp of 0.1 V s^{-1} , which corresponds with a temperature ramp of 2.5 K s^{-1} after calibration. The three systems (Table 1) were characterized and calibrated by using the four calibration samples spanning melting temperatures up to $250 \text{ }^\circ\text{C}$ (Table 2), the Si sample, and by performing probe deflection measurements as a function of the heating voltage applied to the probe while it is free in air (far from contact with a sample). For every sample at least five repeated measurements (each measurement corresponding with a specific location at the sample surface) were performed over a temperature range starting at a temperature below the apparent transition temperature and finishing at a temperature above it. Heating voltage values corresponding to the maximums of probe deflection before the force decreases due to polymer phase changes are compared. In this exercise, it may be noticed that the probe must be quickly removed from the surface just after the detection of a polymeric sample melting to avoid a significant modification of a sample (e.g. producing a hole in the polymeric surface).

The calibration was performed before the measurements of the test samples (Table 3) and the three specimens from Anasys Instruments, and repeated afterwards. Therefore, any significant tip change (due to heating treatment as an example) can be observed. This has been observed in practice rarely; instead it is more common to crash the tip due to a fault in the thermomechanical curve acquisition, e.g. by penetrating too deep inside the material. All the samples (calibration and test samples) were measured with one probe per operator or per compared measurement series.

4. Analysis of the experimental results

To assess the performance of the nano-TA method, the uncertainty of the measurement was estimated and applied to the results obtained in the frame of the inter-laboratory comparison. There are numerous potential uncertainty contributions, related both to calibration of the probe temperature scale and to the thermomechanical response of the samples. Here we briefly discuss the different effects participating in the nano-TA measurement, and suggest the procedure how to estimate their magnitude and contribution to the final uncertainty.

4.1. Uncertainties related to the temperature scale

An important aspect of the uncertainty analysis is that the temperature scale is calibrated using the same method as the measurements on the unknown samples. This helps in reducing many of the potential uncertainty sources related to the thermomechanical response, as

discussed below. However, it adds extra uncertainties related to the temperature scale calibration. In contrast to a heat bath or oven, where we can calibrate probe response for many different temperatures, here we have only few points (in our case four points) and we need to interpolate between them. The following uncertainty sources have been identified:

- **Probe electrical resistance instability:** the probe temperature is obtained from the value of its electrical resistance, however this resistance can change during the experiment (either slow drift out or sudden temperature jump). This can occur for several reasons, but the major effects are related to the laser spot position on the cantilever. By photoelectric effect, the laser produces some extra voltage to the circuit that highly depends on the position of the laser spot on the cantilever, as shown in Fig. 4. On top of it, it produces some heating of the cantilever; however this effect is estimated to be much smaller. When the probe gets heated, it expands and slightly deflects. This effect itself changes the position of the laser spot with respect of the cantilever. Moreover, after heating the probe repeatedly, there can be some residual deformation, leading to systematic shift of the electrical resistance. To thermally stabilize the probe, it is important to ramp the probe far from contact several times before starting the measurements. Moreover, by performing the measurements far from contact before and after the unknown samples measurements, we can estimate the effect of electrical resistance instability.

It is noteworthy that Fig. 4 shows that the polarity of the probe can also play a role. It is therefore recommended to not change this polarity during a calibration and measurement sets.

- **Uncertainty related to the calibration curve fitting.** Typically, the calibration data are fitted using linear or quadratic dependence [19]. The number of calibration samples is usually low (sometimes the same as the number of free parameters in the fit), so it is hard to get the uncertainty via fitting. As an alternative, we can compare the fitting results from the calibration data measured before and after measurements on the unknown samples. This includes even more uncertainty aspects than a simple fitting procedure would allow.
- **Uncertainty of the reference values of the calibration samples.** As explained in section 2.2, samples used in this study were calibrated using traceable DSC devices and the data were provided with expanded uncertainty around 2 K (refer to Tables 2 and 3). However, the DSC method does measure a different physical quantity in a different sample setup, so there can be a systematic error between the SThM results associated to the phase transition temperatures and the DSC data. Indeed, the physical and mechanical properties at the near-to-surface layers of polymer samples, used for SThM measurements, probably differ of those of bulk material properties measured by DSC as they are strongly linked not only to the manufacture (cryo-

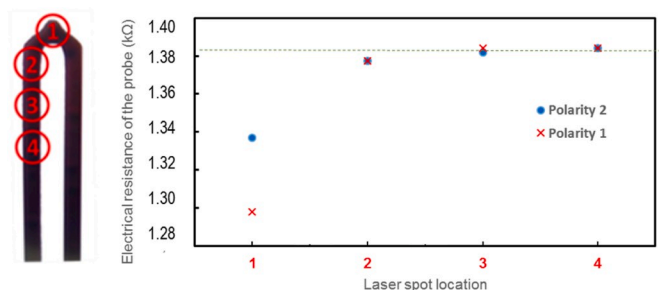


Fig. 4. Electrical resistance of the probe measured using a dc current of 0.1 mA as a function of the laser spot location on the cantilever for the two polarities of the probe in the measurement circuit. Dashed line gives the electrical resistance of the probe while laser is turned off.

ultramicrotomy treatment) but also to the aging of samples, their exposure to light and air for some time before the experiments. Localized oxidation may have taken place and modified the very near-to-surface features. A systematic difference between SThM measurements and DSC measurements could provide an acceptable explanation in the resulting localized modification of the material physical properties.

- **Temperature difference between that measured in the probe and that of the sample surface.** When the probe is heated, heat is partly dissipated into the sample and partly into the cantilever, so a temperature profiles establishes in the probe. There is a significant temperature difference between that measured in the tip, which is averaged over the volume occupied by the electrical resistance in the probe, and that of the sample surface. This is in principle not an issue if the shape of the temperature profiles does not vary from one sample to another. This would require a tip-sample contact similar for all samples and all sample thermal conductivities to be equal. All the samples used in this study were polymers, with thermal conductivities much smaller than the conductivity of Si probe, spanning a limited range of values (see in [Tables 2 and 3](#)). However the values are not identical.

4.2. Uncertainties related to the thermomechanical response

Even if the procedure for system calibration reduces the uncertainties related to the thermomechanical response, there are still some effects to be discussed:

- **Apparent vertical deflection observed when a Si doped probe is heated:** The U shaped cantilever of the DS probes is arched, even when not heated ([Fig. 5 a](#)). The vertical deflection measured when the probe is heated and far from sample (free in air) is the result of the cantilever pre-bending coupled with its longitudinal thermal expansion ([Fig. 5 b](#)). This effect contributes to the measurement when the probe is in contact with a sample but is quite negligible.

4.3. Monte Carlo analysis of the uncertainties

In order to estimate the combined effect of all these phenomena we used the Monte Carlo uncertainty analysis approach [20]. Usually, measurement uncertainties are being treated using the Gauss law of uncertainty propagation. To do so, the measured quantity has to be expressed in form of a model equation that contains all the potential influences and from which the sensitivity to particular uncertainty sources can be obtained by differentiation. In our case the measured quantity is obtained via a set of fitting steps and a maximum search, and this prevents the analytical treatment. In such case the Monte Carlo

uncertainty analysis can be used, by using random realisations of the inputs as obtained from some statistical distribution, running the data evaluation procedure on their combinations and statistically evaluating the result. However, even the shape of the thermomechanical response curve is not analytically known in our case. Therefore, our uncertainty calculation, for every set of measurement on a particular sample, started by using an ideal thermomechanical response curve obtained by averaging multiple experimental curves on this particular sample and by smoothing them. Then, the ideal thermomechanical curve shape was altered using the analytically and numerically known influences of individual uncertainty components (e.g. applying some calibration factor to whole curve or adding the noise of the readout electronics to every point in the curve). Curve maxima for all the altered curves were detected and used as a statistical ensemble of transition temperatures from which both the result value and its uncertainty were obtained. The procedure was repeated for every step of the measurement methodology – starting by the calibration phase and followed by the unknown samples measurement phase. In this way, uncertainties coming from the calibration were passed to the unknown samples measurements.

The whole procedure for obtaining an uncertainty for a single unknown sample result can be summarized as follows:

1. The experimental data for the particular set of measurements were analyzed to obtain the missing uncertainty inputs information, like the electronic noise, thermomechanical curve slope while measuring on silicon and in air, or drift after switching off the feedback, to be used as described below.
2. For each calibration sample measurement data set the idealized thermomechanical curve was constructed by averaging and smoothing the experimental curves obtained on this sample. Using the Monte Carlo procedure, a large number of sets of curves altered by different inputs (adding an electrical noise, altering the slope, etc.) was constructed, the individual curve maxima found and calibration data were obtained from it via fitting each set linearly and obtaining the variance between results from different sets. The calibration uncertainty was further increased by observed differences between calibration before and after unknown samples measurements.
3. For each unknown sample measurement data set the thermomechanical data were treated the same way, now using the calibration data and their uncertainty obtained in the previous step as an extra uncertainty input, used in the phase of generating sets of altered curves. As a result we obtained the uncertainty of the measurement on the particular unknown sample.

The full uncertainty analysis was performed for Device 1 (see [Table 1](#)). This also provided estimates for minor uncertainty components

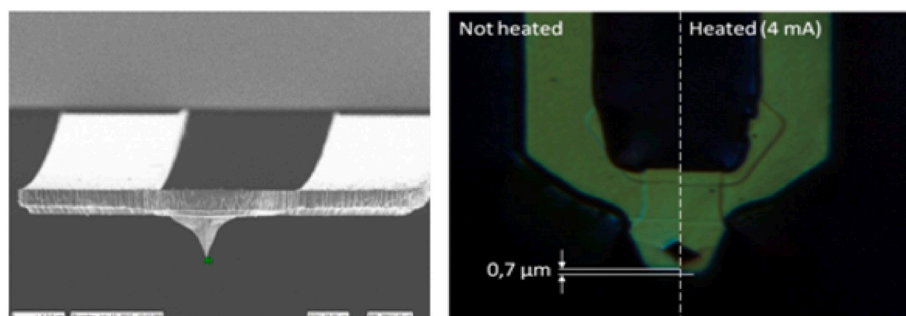


Fig. 5. (a) SEM image of a non-heated DS probe showing that the cantilever is not flat. (b) Two merged optical images of a doped Si probe showing the longitudinal thermal expansion of the cantilever when the probe is not heated (left) and when it is heated (right).

- Uncertainty related to the drift of the deflection signal after switching the feedback off and prior to starting the current ramp. This contributes to the uncertainty of the curve slope: for different curve slopes the maximum can then be at different positions. The drift can be seen in some of the data at the thermomechanical response curve start. It is clearly observed in the response curve of [Fig. 6a](#) obtained for the PCL sample.

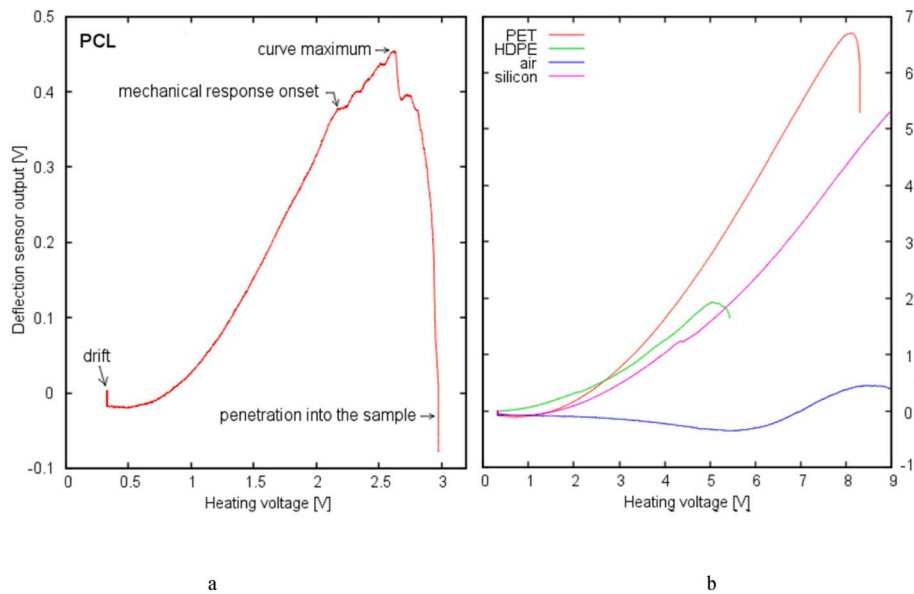


Fig. 6. Examples of thermomechanical response curves showing some typical effects increasing the uncertainty: drift in the thermomechanical response curve start, complex curve shape close to the transition.

- **Uncertainty related to changes of the shape of deflection vs. heating voltage curve:** For a probe free in air (far from contact) or for a measurement on a Si sample (see Fig. 6.b), this is mostly related to the probe deformation while heated. It should ideally be the same for calibration samples and unknown samples measurement, so it does not contribute to the uncertainty. However, this is not the case because two different effects can be seen in different experiments: (i) change of the slope on a smooth curve, e.g. due to the different thermal expansion of the material under test (as illustrated by PET and HDPE curves in Fig. 6. b), which cannot be compensated easily and (ii) complex non-smooth shape of the curve due to some more complex thermomechanical phenomena around the transition temperature (as illustrated in Fig. 6.a) which can be smoothed only by repeating the measurements.
- **Uncertainty related to the difficulty to identify accurately the heating voltage where the phase change occurs.** Some curve shapes are more complex close to the transition temperature, showing some traces of mechanical response at significantly lower heating voltages than where the maximum occurs. An example of this effect is shown in Fig. 6.a. If the transition would be similarly sharp for all the samples, this effect should cancel out by the temperature calibration via reference samples and we would always be comparing the same point on the curve, the maximum. However, if for some of the samples the transition is more complicated or happening on much broader range of heating voltage (i.e. temperatures), this gives an extra systematic error, which would be sample dependent.
- **Electronics readout noise.** The data coming from electronics are in principle noisy, and this effect could slightly alter the estimated position of the curve maximum.

that were then used within experimental data evaluation for all the instruments. Main uncertainty components were evaluated for each measurement individually. Their origin was described in the prior section and whenever possible their numerical values were extracted from the measured data. The following information was used for uncertainty estimation:

- **Uncertainty of reference values** as provided by DSC that are provided in Table 2.
- **Difference of the calibration curve obtained prior and after measurement on unknown samples.** Within Monte Carlo procedure this is added as a variance of the calibration factor, i.e. variance of the slope of calibration curve. The experimentally observed difference of the calibration curve slope before and after the unknown samples measurements was up to 3 percents.
- **Variance of the slope of deflection vs. heating voltage curve.** This is primarily related to the probe bending while heated and was evaluated from data measured far from sample and on silicon surface before and after the measurements. Slope or shape of curve changes were taken into account by adding distortion to the curves generated in Monte Carlo procedure. The observed curve slope change was up to 4% of the slope.
- **Variance of slopes of the deflection signal after switching the feedback off and prior to starting the ramp.** The drift is typically neglected, however as it changes the slope of the curve it can have impact on the maximum position, so it is another slope variance added in the Monte Carlo procedure. Experimentally observed drift was up to 0.05 V per second.
- **Electronics readout noise for steady signal.** This effect was evaluated directly from the raw data obtained by the electronics before starting the ramp. Experimentally observed electrical noise root mean square value was usually very small, around 1 mV.

In addition to these inputs that can be deduced from experiments, we also added extra terms related to long time observations, like the mechanical, electronics and quadrant diode signal drift. However these were found to have negligible impact on the result and it was not necessary to evaluate them for each curve individually.

More than 1000 curves were simulated for determining measurement uncertainty on every sample in order to reach convergence of the results. The resulting uncertainty was between 3 and 5 K, depending on transition temperature value and curve shape (flatness of the maximum). The flatter was the thermomechanical curve maximum the larger was the impact of all the inputs affecting the curve slope. To get an approximate ratio of the sensitivity of final uncertainty on uncertainties of the different inputs, we switched on and off the individual inputs in the calculation procedure. The calibration curve nonlinearity (see also Fig. 7) and difference of the calibration curve prior and after the measurements was found to be the largest contribution, dominating all the other aspects. This is related to the calibration curve fitting, where fitting errors were around 6% of the curve slope. Consequently, it was found that this forms the major contribution to the final uncertainty (about 50% for low transition temperatures, e.g. for PCL and up to 70% for high transition temperatures, e.g. for PET). The next important contributions are the slope variance of thermomechanical curves and reference samples uncertainty (both around 15%). The effect of other influences was marginal, e.g. the mechanical drift after switching the

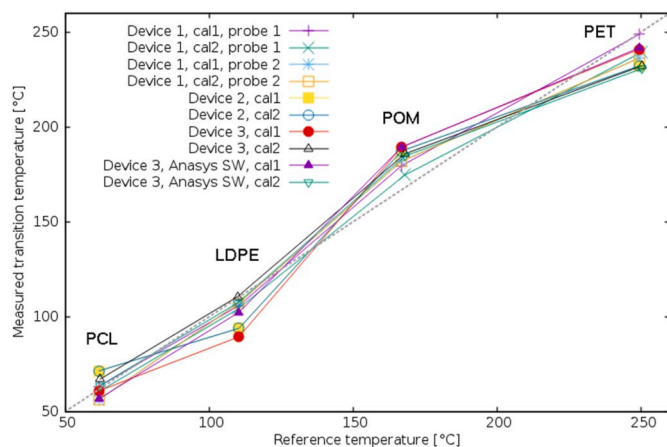


Fig. 7. Comparison between the SThM-determined apparent melting temperatures of the calibration samples after calibration of the probes by fitting and averaging and the DSC-determined reference melting temperatures of the same samples. Data are independently plotted for calibration prior (cal1) and after (cal2) measurements on test samples. The dashed grey line represents the curve $y = x$.

feedback off (2.5% of the uncertainty) or electronics noise effect (up to 0.2% of the uncertainty).

For the data measured with Devices 2 and 3 (Table 1) the experimental contributions discussed above were again used, when available in the experimental data. However, for the minor inputs (e.g. electronics drift), they were kept similar as for Device 1 data, as the major contribution was again the calibration procedure. The uncertainty analysis results (expanded uncertainty) were used for error bars shown in the figures in the next section.

5. Results of the interlaboratory comparison

The data sets for the experiments shown are defined in Table 4, and related to Figs. 7–9 which report the experimental results. All data were obtained in the same way using a simple custom-built software, except data labelled “Device 3 Anasys SW” curves where the automated data evaluation in the microscope software was also used to explore the potential differences between the two data post-processing approaches. Note that the order of samples measured could vary depending on the operator but we did not observe clear dependence on this parameter.

In the calibration steps (cal1 before the measurements of the test samples and cal2 afterwards), probe heating voltages for a given probe and a given device were first averaged. Then a linear fit was used to convert the heating voltage values (V_{hm}) measured on the calibration samples at the apparent phase transitions (peaks or inflections of the deflection curves) were collected. The different voltages V_{hm} were then plotted as a function of DSC temperatures of the reference materials, and a linear fit was made to obtain a way to convert a voltage scale into a temperature one. As the experimental curves of V_{hm} as a function of reference temperature are not perfectly linear, this procedure induces already some uncertainty. In Fig. 7, apparent transition temperature

Table 4
Definition of the data sets shown in Figs. 7–9.

Data set name	SThM device used from Table 1	SThM probe used	Software used
Device 1, probe 1	Device 1	300 μm long	custom-built
Device 1, probe 2	Device 1	200 μm long	custom-built
Device 2	Device 2	200 μm long	custom-built
Device 3	Device 3	200 μm long	custom-built
Device 3, Anasys SW	Device 3	200 μm long	Anasys

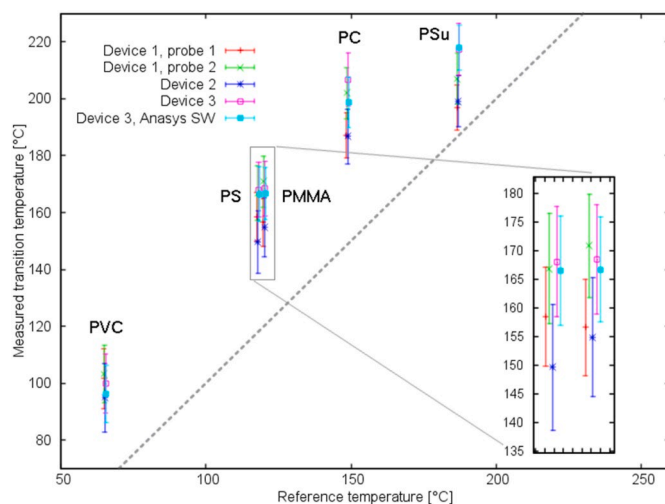


Fig. 8. SThM-determined apparent phase-transition temperatures as a function of the calibrated temperature scale. Results on the 5 test samples (Table 3), including different probes and different evaluation methods. Error bars are showing the expanded uncertainty ($k = 2$). Points are slightly mutually shifted in the x-axis direction for better visibility. The dashed grey line represents the curve $y = x$.

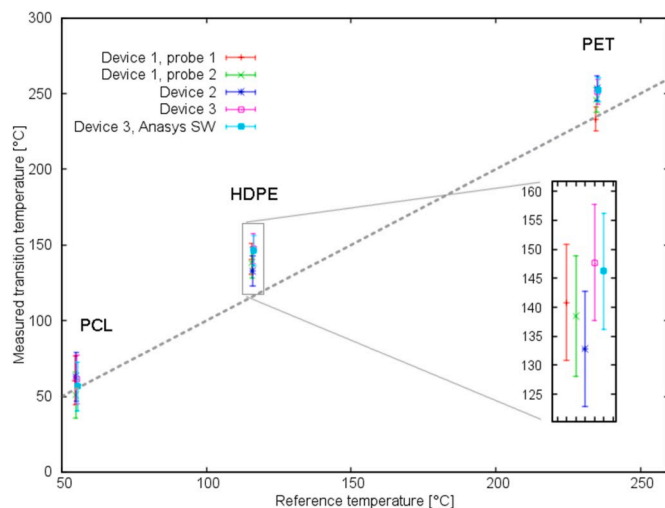


Fig. 9. SThM-determined apparent melting temperatures of the Anasys calibration samples, including different probes and different evaluation methods, following temperature calibration with the references samples considered in this work. Error bars are showing the expanded uncertainty ($k = 2$). Points are slightly mutually shifted in the x-axis direction for better visibility. The dashed grey line represents the curve $y = x$.

$T_{at,SThM}$ values obtained by SThM and measured with this procedure are represented as a function of the T_m values measured using DSC (reference temperatures). It is found that the results obtained by the different devices have a similar “S” shape. This demonstrates that calibration data cannot be fitted by a quadratic curve in the calibration step, as suggested by Anasys Instruments [20]. For given device and sample, the deviation between the apparent melting temperatures ($T_{am,SThM}$) estimated from cal1 and cal2 can be up to ± 20 K. For a given sample, the maximum difference between temperatures measured with SThM devices is of the same order of magnitude, ± 20 K, and the maximum deviation obtained between SThM temperatures and DSC reference temperatures can reach ± 30 K. As previously discussed linearity and repeatability of data calibration appears to be a large source of uncertainty.

Figs. 8 and 9 provide the results obtained with the test samples and

with the samples provided by Anasys Instruments, respectively. In both cases, data obtained with calibration prior (cal1) and after (cal2) the measurements are displayed. In Fig. 8, $T_{at,SThM}$ temperature measurements on the amorphous test samples obtained using calibrated SThM probes are given as a function of the T_g measured by DSC (indicated in Table 3). As for the calibration data the maximum difference between temperatures measured with SThM devices is about 20 K (if we do not take into account the expanded uncertainty). Furthermore, we can observe that all the values of $T_{at,SThM}$ are larger than those obtained by DSC whatever the device used. For a given sample, the difference of temperature between SThM data and DSC measurements varies from 10 to 50 K. Such results have already been reported in literature [21,22], whereby SThM-detected phase-transition for amorphous materials is detected at a temperature larger than that expected and is related to an alteration in thermal contact between the sample and probe caused by sample flow due to softening. Consequently, these results and our results for amorphous materials can be reasonably ascribed to sample flow rather than the T_g itself.

Our results also show that the signature of the phase transition for amorphous materials is less pronounced and less sharp in the curves than that for semi-crystalline materials. This is a result of the two different processes involved (melting and putative softening). For the latter a very abrupt deflection downward in the deflection curves is observed at the melting. The transition associated with amorphous materials is more smooth and continuous. In the case of the softening transition associated with glassy materials, the continuous deflection reflects the disordered and disperse nature of this phase. This leads to a larger uncertainty for amorphous materials than for semi-crystalline materials.

Fig. 9 summarises the apparent melting temperatures obtained by SThM for the three Anasys calibration samples and compares these data to the 'exact' melting temperatures (data provided by Anasys Instruments). Here, the temperatures measured using SThM can be of 36 K larger than the T_m reference temperatures. Once more, similar to the calibration data, the maximum difference between temperatures measured with SThM devices is about ± 20 K.

For Figs. 8 and 9, we note that there is a small difference (2 K at maximum) between temperatures estimated manually and those using the Anasys Instruments software, probably caused by slightly different evaluation procedures. It is therefore important in practice to keep the evaluation method consistent across the calibration and unknown samples measurement.

6. Conclusions, recommendations and perspectives

SThM is assessed as a method for determining the local phase transition temperature of polymeric materials by means of nano-TA. Semi-crystalline and amorphous polymers that were characterized first using DSC are used as reference and tests samples respectively. The surface of these samples that come from the same raw materials than those used for DSC measurements were prepared for nano-TA measurements using cryo-ultramicrotomy to minimize their roughness and are studied by nano-TA, in the temperature range 50–250 °C. The repeatability, the reproducibility and the reliability of nano-TA are evaluated by three laboratories applying the same protocol. The calibration of the probe temperature scale and the variability of the sample thermomechanical response are included in a Monte Carlo uncertainty analysis, resulting in uncertainty between 3 and 5 K. The comparison of the temperatures identified using the deflection of the SThM probe when local phase transitions are detected with DSC-measured phase-transition temperatures for the semi-crystalline samples rule out the possibility of a quadratic fit and call for a linear calibration in absence of any additional information. The maximum deviation obtained between apparent phase transition temperatures measured using nano-TA and DSC temperatures with such linear calibration reaches ± 30 K for semi-crystalline samples and 50 K for amorphous samples. The deviation could result from

differences between nano-TA and DSC. Physical properties at the near-to-surface layers of calibration and test polymer samples probably differ of those of bulk material as surface properties are strongly linked to the manufacture and the aging of samples. The deviation difference is the result of the two different processes involved: melting and putative softening respectively. Furthermore, the transition associated with amorphous materials is more smooth and continuous than for semi-crystalline materials.

The main observations are that the uncertainty on the measurements is larger than what initially thought when using nano-TA in its simplest and widely used methodology (calibration by performing thermo-mechanical curves on the calibrations samples and fitting the results) and only apparent and indicative phase transition temperatures can be measured. A better methodology based on a comprehensive modelling of the probe response and the phenomena involved in local measurements is required.

In addition to the observations made higher, we would like to point to some key issues. First, from a practical point of view, peaks observed at the phase transition point can be unclear and sometimes multiple, especially for the lowest temperatures, which slightly increases the measurement uncertainty. Let us notice that the use of derivative curves may reduce this uncertainty allowing a more accurate determination of the maxima of probe deflection at the phase transitions. When setting the AFM optical deflection measurement system before nanoTA calibration, it is recommended to verify that the maximum deflection corresponding to the highest melting temperature can be detected.

Second, within the calculated uncertainties the results obtained by the three different instruments used are in agreement but systematic deviation and therefore uncertainty is much larger than originally anticipated. Linearity and repeatability of data calibration is the main source of uncertainty. However, primary source of the calculated uncertainty remains unknown. The calibration could be improved by better choice of samples, however the repeatability (drift of calibration coefficients) remains problematic and this already increases the uncertainty by a few kelvins. This effect could be related to probe contamination, which can be significant after approximately 50 indentations into various plastics. It is suggested that the probe can be cleaned by heating far from sample, e.g. in air [20]. However this changes sometimes the electrical properties, so it should not be performed within a single experiment to keep the data consistent. A change in the electrical properties of the probe would induce a different electro-thermal behaviour of the probe. The used probe geometry (cantilever length), electronics and curve maximum search procedure have no impact on the result (within the large uncertainty).

Finally, on basis of these measurements, we remind that the initial measurement protocol was improved by adding the second calibration set measurements after unknown samples measurement. It is also recommended to measure the drift, which may not be possible for commercial devices but can be done manually. Also the checks far from sample (in air) and on silicon substrate are important to eliminate potential uncertainty related to probe properties change. We note that probe calibration in an oven is not necessarily useful as the probe resistance depends highly on the laser position on the cantilever. It is not recommended to remove or realign the probe during the experiment - all the data should be measured under exactly same conditions and with exactly same probe.

Declaration of competing interest

The authors declare that they have no known competing financial interests or personal relationships that could have appeared to influence the work reported in this paper.

Acknowledgements

The research leading to these results has received funding from the

European Union Seventh Framework Program FP7-NMP-2013-LARGE-7 under grant agreement n°604668 (QUANTIHEAT).

We thank the Centre Technologique des Microstructures (CTμ), Lyon, France for the preparation of the surface of the calibration and test polymeric samples. This project has received partial funding from the European Union's Horizon 2020 research and innovation programme under grant agreement GrapheneCore2 785219 number. The work has also been financially supported by the Department for Business, Energy and Industrial Strategy through NMS funding (2D Materials Cross-team project) and by the Ministries of Europe and Foreign Affairs and Higher Education, Research and Innovation through Barrande program and by project CEITEC 2020 under No. LQ1601.

Appendix A. Supplementary data

Supplementary data to this article can be found online at <https://doi.org/10.1016/j.ijthermalsci.2020.106502>.

References

- [1] G.J. Georges, M.S. Sreekala, S. Thomas, A review on interface modification and characterization of natural fiber reinforced plastic composites, *Polym. Eng. Sci.* 41–9 (2001) 1548–2634.
- [2] K. Lau, C. Gu, D. Hui, A critical review on nanotube and nanotube/nanoclay related polymer composite materials, *Compos. B Eng.* 37–6 (2006) 425–436.
- [3] S. Ganguli, A. K Roy, D. P Anderson, Improved thermal conductivity for chemically functionalized exfoliated graphite/epoxy composites », *Carbon* 46–5 (2008) 1873–3891.
- [4] S. Gomès A, P.O. Assy, Chapuis Scanning thermal microscopy: a review, *Phys. Status Solidi* 3 (2015) 477–494.
- [5] A. Hammiche, M. Reading, H.M. Pollock, M. Song, D.J. Hourston, Localized thermal analysis using a miniaturized resistive probe, *Rev. Sci. Instrum.* 67 (1996) 4268–4274.
- [6] Nelson, W.P. King, Measuring material softening with nanoscale spatial resolution using heated silicon probes, *Rev. Sci. Instrum.* 78 (2007), 02370.
- [7] M.H. Li, Y.B. Gianchandani, Microcalorimetry Applications of a surface micromachined bolometer-type thermal probe, *J. Vac. Sci. Technol. B* 18 (2000) 3600–3603.
- [8] H.M. Pollock, A. Hammiche, Micro-thermal analysis: techniques and applications, *J. Phys. D Appl. Phys.* 34 (2001) R23–R53.
- [9] R. Hler, E.z. Mhlen, An introduction to MTATM and its application to the study of interfaces, *Thermochim. Acta* 361 (2000) 113–120.
- [10] M.S. Tillman, B.S. Hayes, J.C. Seferis, Examination of interphase thermal property variance in glass fiber composites, *Thermochim. Acta* 392–393 (2002) 299–302.
- [11] L. Germinario, P. Shang, Advances in nano thermal analysis of coatings, *J. Therm. Anal. Calorim.* 93–1 (2008) 207–211.
- [12] T. Souier, Y.A. Samad, B.S. Lalia, R. Hashaikeh, M. Chiesa, Nanoscale thermal analysis of multiphase polymer nanocomposites, *J. Phys. Chem. C* 116 (2012) 8849–8856.
- [13] P. Rivière, T. Nypelö, O.J. Rojas, A. Klug, N. Mundigle, R. Wimmer, Space-resolved thermal properties of thermoplastics reinforced with carbon nanotubes, *J. Therm. Anal. Calorim.* 127–3 (2017) 2059–2074.
- [14] V.V. Gorbunov, D. Grandy, M. Reading, V.V. Tsukruk, D. Joseph, R. Mencil, B. PrimeA, Micro and nanoscale local thermal analysis, 615-649. Book: *Thermal Analysis of Polymers, Fundamentals and Applications*, John Wiley & Sons, INC. PUBLICATION, 2008.
- [15] Quantiheats Good Practice Guide, 2018.
- [16] <https://www.bruckerfmprobes.com/a-3698-vita-cs-nanota.aspx>.
- [17] S. Gomès, A. Assy, P.O. Chapuis, L. Carlos, F. Palacio, Scanning thermal microscopy. Book: *Thermometry at the Nanoscale – Fundamentals and Selected Applications*, Royal Society Publishing 75–314, 2015.
- [18] M. Yavari, S. Maruf, Y. Ding, H. Lin, Physical aging of glassy per fluoropolymers in thin film composite membranes. Part II. Glass transition temperature and the free volume model, *J. Membr. Sci.* 525 (2017) 399–408.
- [19] Nano Thermal Analysis, Anasys Instruments manual, 2009.
- [20] GUM supplement: ISO/IEC. Propagation of distributions using a Monte Carlo method, International Organization for Standardization, Geneva, Switzerland, 2008. ISO/IEC 98–3:2008/Suppl1:2008.
- [21] P.G. Royall, V.L. Kett, C.S. Andrews, Identification of crystalline and amorphous regions in low molecular weight materials using microthermal analysis, *J. Phys. Chem. B* 105 (2001) 7021–7026.
- [22] P.G. Royall, V.L. Hill, D.Q. Craig, D.M. Price, M. Reading, An investigation into the surface deposition of progesterone on poly (d, l-) lactic acid microspheres using micro-thermal analysis, *Pharmaceut. Res.* 18–3 (2001) 294–298.